

Cell Reports, Volume 27

Supplemental Information

STRIPAK Members Orchestrate Hippo and Insulin

Receptor Signaling to Promote

Neural Stem Cell Reactivation

Jon Gil-Ranedo, Eleanor Gonzaga, Karolina J. Jaworek, Christian Berger, Torsten Bossing, and Claudia S. Barros

Supplemental Figures and Figure Text

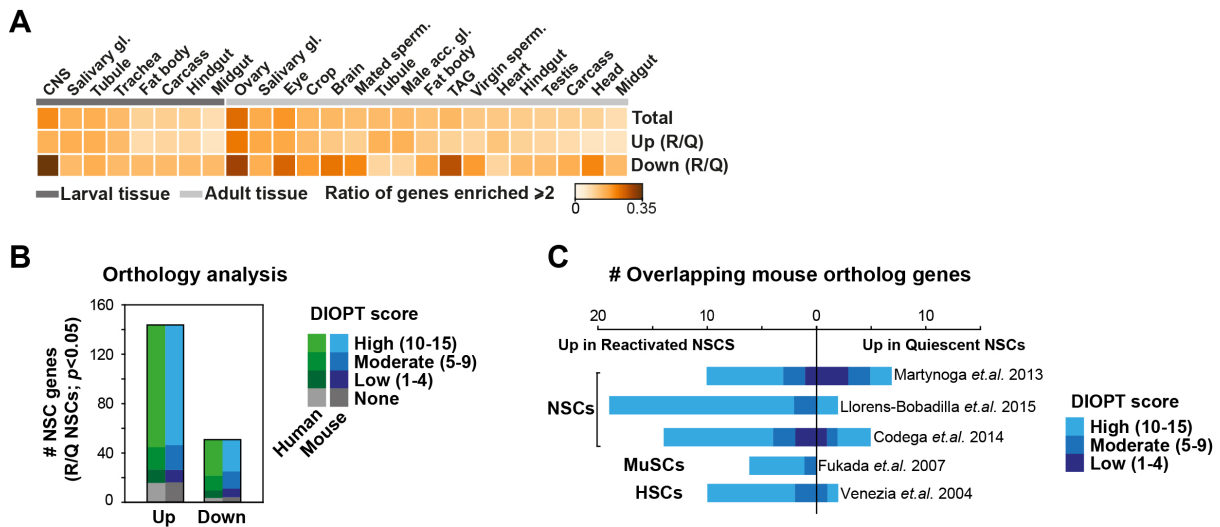


Figure S1, related to Figure 1. Tissue expression enrichment and orthology conservation of identified targets in transcriptome analysis. (A) Heatmap depicting identified larval and adult tissue-specific gene sets enriched by a minimum of 2-fold to expression in whole fly. gl: gland. Sperm: spermatheca; acc: accessory; TAG: thoracoabdominal ganglion. See also Table S2. **(B)** Number of human and mouse orthologues (single best matches) of identified genes grouped by orthology score (DIOPT) (Hu, et al., 2011). See also Table S1. **(C)** Number of identified genes with mouse orthologues (single best matches) reported upregulated in quiescent or proliferating mouse embryonic or adult NSCs, skeletal muscle satellite stem cells (MuSCs) and hematopoietic stem cells (HSC). DIOPT score groups indicated. See also Table S3. The data used for the above assays comprise targets identified in our transcriptome analysis as up- or downregulated in reactivating (R) versus quiescent (Q) NSCs (limma moderated t -test, $p < 0.05$).

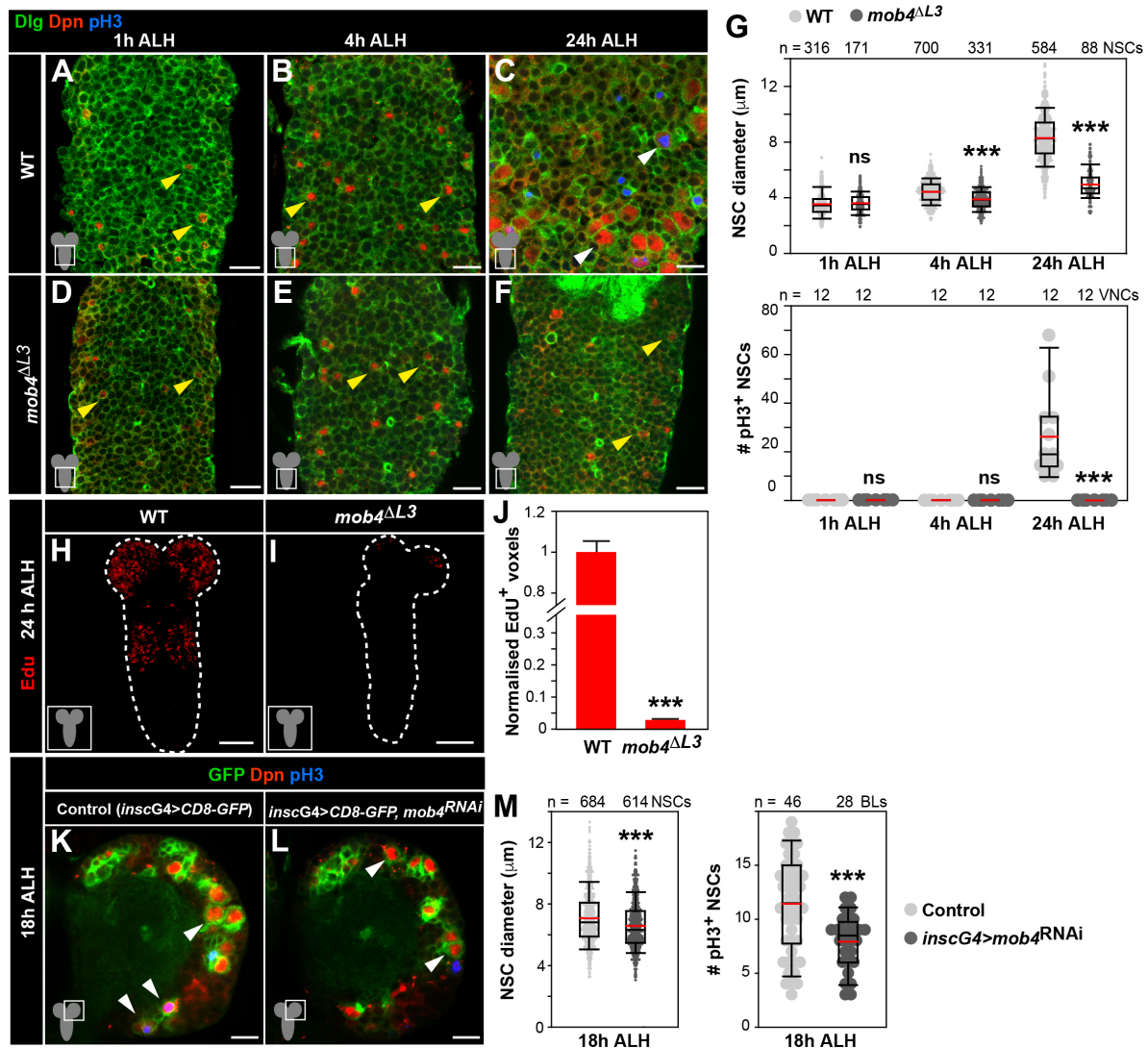


Figure S2, related to Figure 2. NSC reactivation defects upon Mob4 loss or inhibition. (A-G) NSC enlargement and division is impaired in *mob4* mutant ventral nerve cords (VNCs). VNCs of WT (A, 1h ALH; B, 4h ALH; C, 24h ALH) and *mob4*^{ΔL3} (D, 1h ALH; E, 4h ALH; F, 24h ALH). NSCs in red (Dpn), cell membranes in green (Dlg), divisions in blue (pH3). Yellow and white arrowheads indicate quiescent and reactivated NSC examples, respectively. Scale bar: 10 μm. Anterior up. (G) Quantification of NSC diameters (1h ALH: WT n=316 NSCs, 7 VNCs; *mob4*^{ΔL3} n=171 NSCs, 5 VNCs. 4h ALH: WT n=700 NSCs, 6 VNCs; *mob4*^{ΔL3} n=331 NSCs, 5 VNCs. 24h ALH: WT n=584 NSCs, 5 VNCs; *mob4*^{ΔL3} n=88 NSCs, 8 VNCs) and proliferation (1h ALH: WT n=12 VNCs; *mob4*^{ΔL3} n=12 VNCs. 4h ALH: WT n=12 VNCs; *mob4*^{ΔL3} n=12 VNCs. 24h ALH: WT n=12 VNCs; *mob4*^{ΔL3} n=12 VNCs). (H-J) NSCs in *mob4* mutant larval brains do not enter S-phase, except the MbNSCs. WT (H) and *mob4*^{ΔL3} (I) CNSs at 24hph Edu-labelled (red). (J) Quantification of Edu⁺

voxels from CNSs, normalized to controls (WT n=7 CNSs, *mob4*^{ΔL3} n=8 CNSs; error bars: s.e.m). Scale bar: 50μm. (K-M) NSC-specific expression of *mob4*-RNAi results in a small reduction in cell size and decreased number of NSCs in division. Brain lobes (BLs) of control (K, *insc-gal4>CD8-GFP*) and *mob4*-RNAi expressing brains (L, *insc-gal4> CD8-GFP, mob4*^{RNAi}) at 18h ALH. NSCs in green (*CD8-GFP*, GFP) and red (Dpn), divisions in blue (pH3). Arrowheads: NSC examples. Anterior up. Scale bar: 10μm. (M) Quantification of NSC diameters (*insc-gal4>CD8-GFP*, n=684 NSCs, 9 BLs, 9 brains; *insc-gal4> CD8-GFP, mob4*^{RNAi} n=614 NSCs, 8 BLs, 8 brains) and divisions (*insc-gal4>CD8-GFP*, n=46 BLs, 23 brains; *insc-gal4> CD8-GFP, mob4*^{RNAi} n=28 BLs, 14 brains). Wilcoxon rank sum tests, ****p*<0.001, *p*>0.05: non-significant (ns).

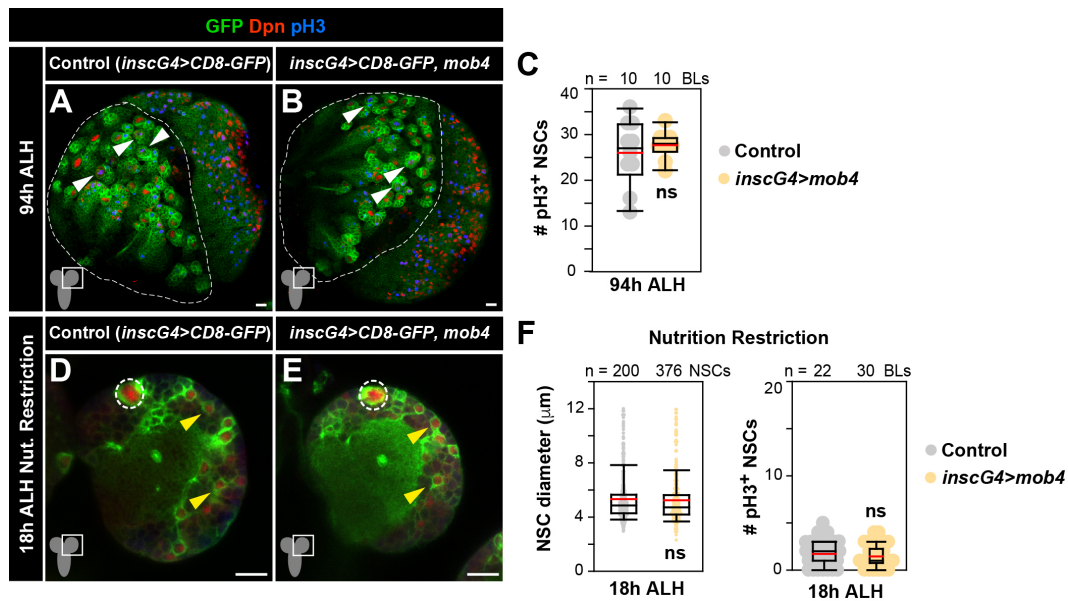


Figure S3, related to Figure 3. *Mob4* overexpression does not lead to NSC overproliferation nor induces NSC reactivation under nutrition restriction.

NSC-specific *mob4* overexpression does not affect NSC proliferation in late larval brains (A-C) nor promotes reactivation of NSCs in larvae deprived of amino acids (sucrose-only diet; D-F). Brain lobes (BLs) of control (A, D, *insc-gal4>CD8-GFP*) and *mob4* overexpressing brains (B, E, *insc-gal4>CD8-GFP, mob4*) at 94h (A, B) and 18h ALH (D, E). NSCs in green (GFP) and red (Dpn), divisions in blue (pH3). Dashed line: central brain region. White arrowheads: dividing NSC examples. Yellow arrowheads: quiescent NSC examples. Dashed circles: MbNSCs. Scale bar: 10 μ m. Anterior up. (C) Quantification of NSC divisions (94h ALH: *insc-gal4>CD8-GFP* n=10 BLs, 10 brains; *insc-gal4>CD8-GFP, mob4* n=10 BLs, 10 brains). (F) Quantification of NSC diameters (18h ALH: *insc-gal4>CD8-GFP* n=200 NSCs, 6 BLs, 5 brains; *insc-gal4>CD8-GFP, mob4* n=376 NSCs, 5 BLs, 5 brains) and divisions (18h ALH: *insc-gal4>CD8-GFP* n=22 BLs, 16 brains; *insc-gal4>CD8-GFP, mob4* n=30 BLs, 16 brains). Wilcoxon rank sum tests, $p>0.05$: non-significant (ns).

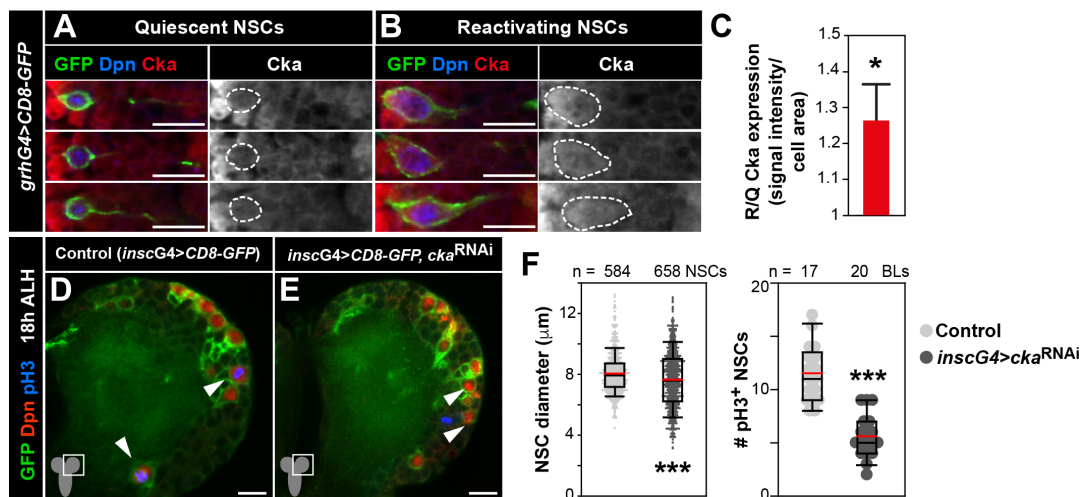


Figure S4, related to Figure 5. Cka inhibition delays NSC growth and division.

(A-C) Cka is upregulated in reactivating (R) compared with quiescent (Q) NSCs. Examples of quiescent (small; A) and reactivating (enlarged, B) NSCs in 17h ALH brains (VNC thoracic region) labelled with *grh-Gal4* driving *CD8-GFP* (GFP, green), Cka (red) and Dpn (blue). Cka channel also shown in monochrome. Dashed lines: cell bodies. (C) Cka protein quantification in reactivating normalised to quiescent NSCs (n= 20 reactivating NSCs and n=20 quiescent NSCs, 20 BLs, 10 brains; error bars: s.e.m.; Wilcoxon rank sum test, * $p < 0.05$). (D-F) NSC-specific expression of *cka-RNAi* results in reduced cell size and decreased number of NSCs in division. Brain lobes (BLs) of control (D, *insc-gal4>CD8-GFP*) and *cka-RNAi* expressing brains (E, *insc-gal4> CD8-GFP, cka^{RNAi}*) at 18h ALH. NSCs in green (*CD8-GFP*, GFP) and red (Dpn), divisions in blue (pH3). Arrowheads: NSC examples. Anterior up. Scale bar: 10 μ m. (F) Quantification of NSC diameters (*insc-gal4>CD8-GFP*, n=584 NSCs, 8 BLs, 4 brains; *insc-gal4> CD8-GFP, cka^{RNAi}* n=658 NSCs, 8 BLs, 4 brains) and divisions (*insc-gal4>CD8-GFP*, n=17 BLs, 9 brains; *insc-gal4> CD8-GFP, cka^{RNAi}* n=20 BLs, 10 brains). Wilcoxon rank sum tests, *** $p < 0.001$.

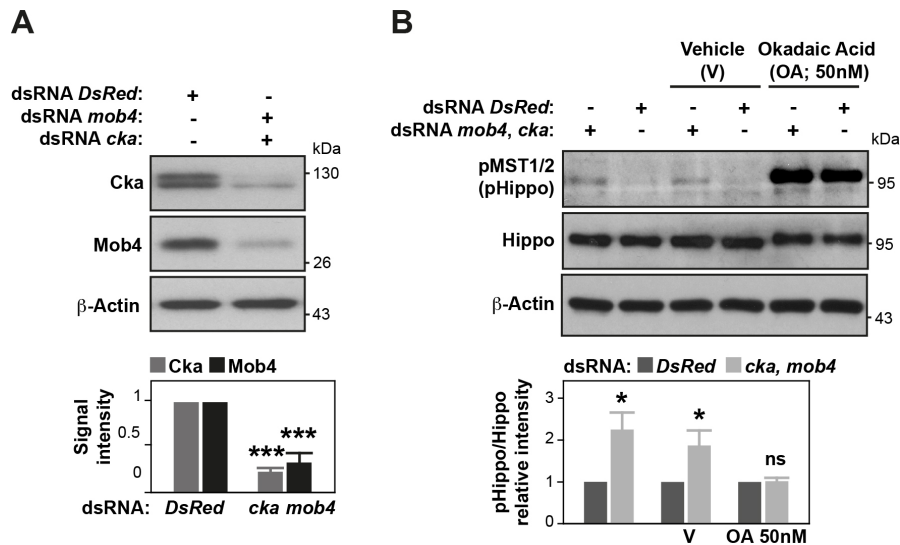


Figure S5, related to Figure 5. Inhibition of Mob4 and Cka increase Hippo phosphorylation. (A) Efficiency of *mob4* and *cka* RNAi-mediated depletions used in *Drosophila* S2R+ assays. dsRNAs targeting *mob4* or *cka*, but not *DsRed* control, lead to depletion of Mob4 and Cka proteins. Lysates analysed with indicated antibodies. β -Actin: loading control. Quantification of Mob4 and Cka signal intensities normalised to control (*DsRed* RNAi) levels (lower panel; n=3 independent assays; error bars: s.e.m; Student's *t*-tests, *** $p < 0.001$). (B) Mob4/ Cka depletion leads to increased levels of activated (phosphorylated) Hippo (pHippo) in S2R+ cells, consistent with published studies (Zheng, et al., 2017; Liu, et al., 2016; Ribeiro, et al., 2010). *Drosophila* S2R+ cells treated with dsRNAs targeting *mob4* and *cka* or control *DsRed*, as well as in the presence of vehicle (0.0005% DMSO) or Okadaic acid (OA) as a positive control for hippo phosphorylation. Lysates analysed by western-blot with indicated antibodies. β -Actin: loading control. Note the total Hippo band mobility shift due to hyperphosphorylation in OA-treated samples. Quantification of pHippo levels shown as mean of the ratio between pHippo and total Hippo signal intensities relative to control (*DsRed* RNAi) levels (lower panel; n=3 independent assays; error bars: s.e.m; Student's *t*-tests, $p^* < 0.05$, $p > 0.05$: non-significant, ns).

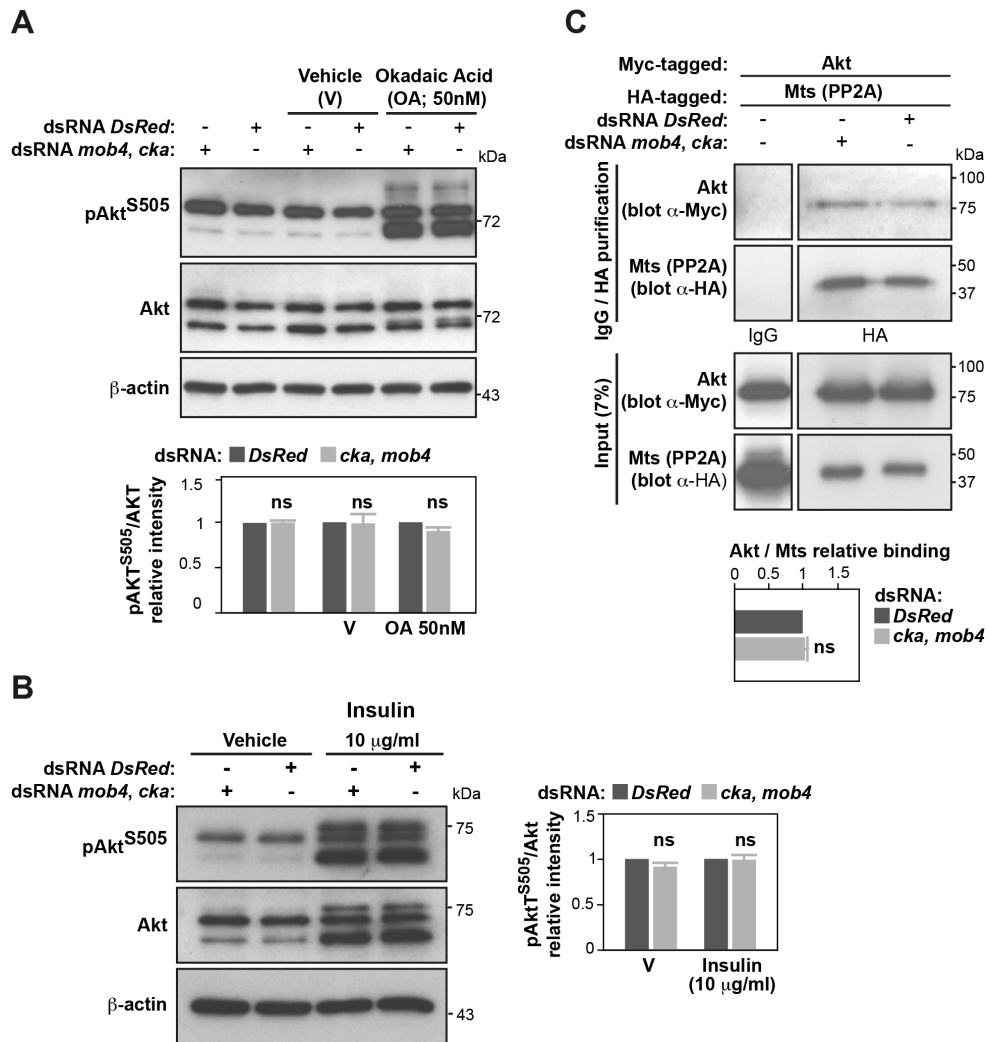


Figure S6, related to Figure 5. Inhibition of Mob4 and Cka does not affect Akt phosphorylation nor the association of PP2A/Mts to Akt. (A, B) Depletion of *mob4* and *cka* has no effect in the levels of activated (phosphorylated) Akt (pAkt^{S505}) in S2R+ cells (A) with or without stimulation with Insulin (B). (A) *Drosophila* S2R+ cells treated with dsRNAs targeting *mob4* and *cka* or control *DsRed*, as well as in the presence of Okadaic acid (OA) as a positive control for Akt phosphorylation or vehicle (V). Lysates analysed with indicated antibodies. β-Actin: loading control. Quantification of pAkt levels shown as mean of the ratio between pAkt and total Akt signal intensities relative to control (*DsRed* RNAi) levels (lower panel; n=3 independent assays). (B) RNAi-mediated depletion of *mob4* and *cka*, or control *DsRed*, in S2R+ cells treated with Insulin or vehicle. Lysates analysed by western-blot with indicated antibodies. β-Actin: loading control. Quantification of pAkt levels shown as mean of pAkt/ Akt signal intensity ratios relative to control (*DsRed* RNAi) levels (right panel; n=3 independent assays). (C) Co-IP assays using S2R+ cells

expressing Myc-Akt and HA-Mts, in addition to RNAi against *mob4* and *cka* or control *DsRed*. Lysates and HA-purified immunoprecipitates analysed by western-blot with indicated antibodies. Negative control co-IP performed using rat IgG instead of rat anti-HA antibody. Quantification of relative binding of Myc-Akt to HA-Mts shown as mean of the ratio between Myc-Akt and HA-Mts signal intensities relative to control (*DsRed* RNAi) levels (lower panel; n=3 independent assays). Error bars: s.e.m. Wilcoxon rank-sum tests, $p>0.05$: non-significant (ns).

Supplemental Table

Gene (Symbol)	Forward Primer (5'→3')	Reverse Primer (5'→3')	Source
<i>ase</i>	CACCTACCAACTGCTGACG	GCTGCTGCTGCTAATGTTG	This paper
<i>dpn</i>	CGCTATGTAAGCCAAATGGATGG	CTATTGGCACACTGGTTAAGATGG	(Berger, et al., 2012)
<i>rheb</i>	TGAGGTGGTGAAGATCATATACGAA	GCCAGCTTCTTGCCTTCCT	(Zitserman, et al., 2012)
<i>cka</i>	GGAGACGGAAGGCGTCAT	TCTCGTCGTCGGACATC	This paper
<i>CG10903</i>	GAGTCTCGGTTGATTTTGGACA	TCTCCAGAATGACATCCCA	This paper
<i>asf1</i>	GGGCGACACATCTTTGTCTTC	GCAGGTAAGCAGAACAATGGTAA	This paper
<i>Gbeta13F</i>	TGGTGGCTATCTATCGTGCTG	GCCCCAAAACGAGGTTACCTG	This paper
<i>phax</i>	ATGATGGAAGTGCACGCAAT	CAGGTGGTAAGGGGACTGG	This paper
<i>NiPp1</i>	ATGGCTAACAGCTACGACATACC	TGTTGCGACCAAATAGATAGCAT	This paper
<i>mob4</i>	TGGGCACGATCAGATTCTCC	CATCTTCTCGCACGCTACT	This paper
<i>crc</i>	GAAACTGGGAGGATACGTGG	GAGAGGTCTGAATGCCTTTGTC	This paper
<i>bet3</i>	ATGTCACGACAAGCCTCTCG	GAGTGCTCCGTAGGTGAGT	This paper
<i>ed</i>	GATGAGCTCCTGTTCTCCGG	GTTGGAATCGCAATGGTCGG	This paper
<i>pdp1</i>	AATCCCATTACCAGCGCAA	GGCATTCCCATTGATCCCT	This paper
<i>how</i>	AACTTTGTGCGTGCATTTT	CGTCCTCCTTCTTGTGCG	This paper
<i>p120ctn</i>	AACATGGACCTTTTATTGACGC	ATATCCTGCTGCCGAAAATTGA	This paper
<i>Rip11</i>	TGGAGTCCGACGCACTGTA	CAATGGTGACGAAGCAGTTGT	This paper
<i>l(2)35Df</i>	CATCGAAAGAAGCTACATCCTCC	GTGGGTTTCGTCATCTGCATTAT	This paper
<i>nito</i>	ACAAGAAGTTTGGCGATTTTAGC	CTTCAGGCGTTTCGGAAGCAA	This paper
<i>mts</i>	TCCAGTTCATAAGAGCCGC	CACGATCGCAATGTGGTCAC	This paper
<i>rp49</i> (calibrator)	GCTAAGCTGTCGCACAAATG	GTTCGATCCGTAACCGATGT	(Kohyama-Koganeya, et al., 2008)

Table S4, related to STAR Methods. Primers used for real-time quantitative PCR assays.